Influence of spin-orbit coupling on the electron-phonon renormalized electronic energy levels in polar materials

Véronique Brousseau-Couture[1], Michel Côté [1], Xavier Gonze [2,3]

Abidev 2021, June 3rd 2021

[1] Département de Physique, Université de Montréal and RQMP, Montréal, Québec, Canada
[2] Université Catholique de Louvain and IMCN/NAPS, Louvain-la-Neuve, Belgium
[3] Skolkovo Institute of Science and Technology, Moscow, Russia

Predominance of non-adiabatic effects in polar materials

Origin of this work:

- <u>Goal</u>: **Systematic**, **larger scale** study of non-adiabatic effects on ZPR (30 materials)
- <u>Conclusions</u>:
  - ∗ Essential for agreement with experiment
  - ∗ Long-range Fröhlich interaction: **slow response** of electrons to **fast LO phonons** dominates ZPR

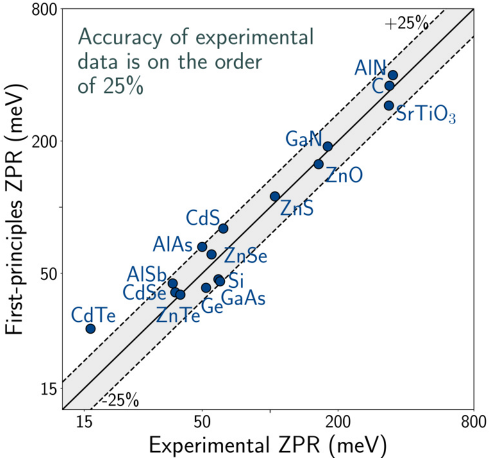

Adapted from Miglio, Brousseau-Couture *et al.*, NPJ Computational Materials **6** 167 (2020)

Predominance of non-adiabatic effects in polar materials

Origin of this work:

- Goal: **Systematic**, **larger scale** study of non-adiabatic effects on ZPR (30 materials)
- Conclusions:
  - ∗ Essential for agreement with experiment
  - ∗ Long-range Fröhlich interaction: **slow response** of electrons to **fast LO phonons** dominates ZPR

How does SOC affect the Fröhlich interaction and ZPR?

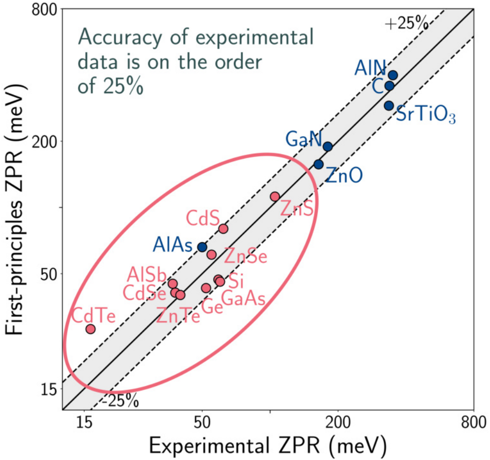

Adapted from Miglio, Brousseau-Couture *et al.*, NPJ Computational Materials **6** 167 (2020)

Effect of SOC on electronic structure

Zinc-blende structure:

- Degeneracy lifted: $\Gamma_4 \rightarrow \Gamma_8 \oplus \Gamma_7$

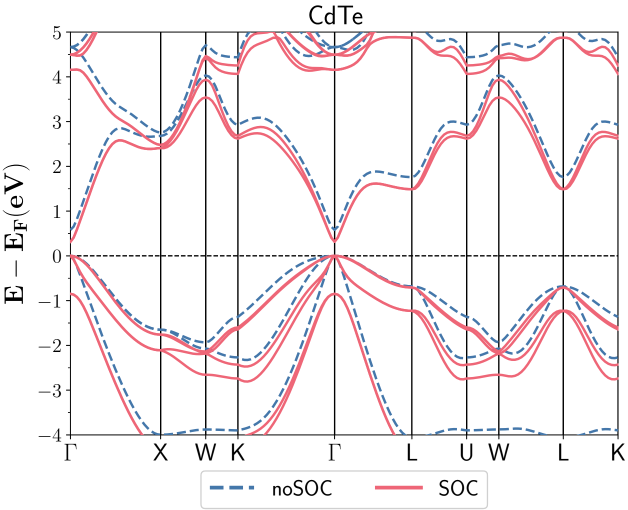

Effect of SOC on electronic structure

Zinc-blende structure:

- Degeneracy lifted: $\Gamma_4 \rightarrow \Gamma_8 \oplus \Gamma_7$
- Global lowering of $\varepsilon_{\boldsymbol{k}n}$ (occupied bands)

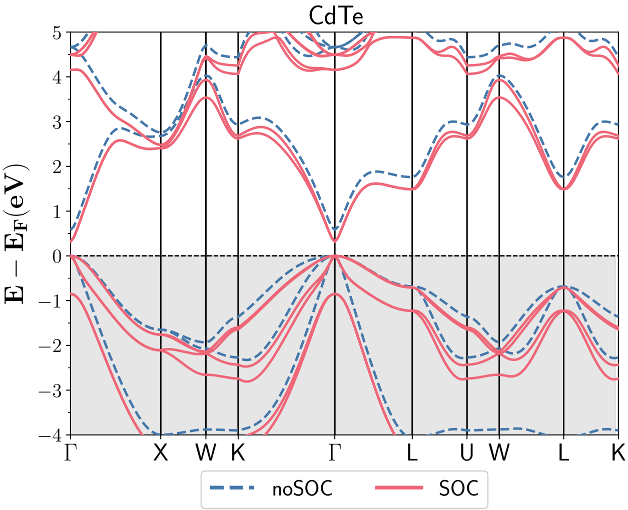

Effect of SOC on electronic structure

Zinc-blende structure:

- Degeneracy lifted: $\Gamma_4 \rightarrow \Gamma_8 \oplus \Gamma_7$
- Global lowering of $\varepsilon_{\boldsymbol{k}n}$ (occupied bands)
- Modification of effective masses

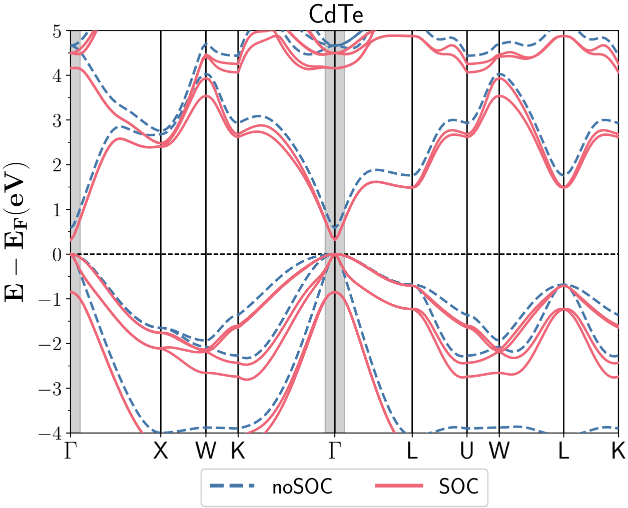

Effect of SOC on electron-phonon interaction

Renormalized eigenenergies :

$$\varepsilon_{\boldsymbol{k}n}(T) = \varepsilon^0_{\boldsymbol{k}n} + \mathfrak{Re}[\underbrace{\Sigma^{\text{EPI}}_{\boldsymbol{k}n}(T,\omega)}_{\text{Self-energy}}]$$

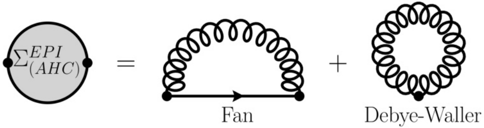

Non-adiabatic AHC Fan self-energy:

$$\Sigma^{\text{Fan}}_{\boldsymbol{k}n}(T=0) = \frac{1}{N_{\boldsymbol{q}}} \sum_{\boldsymbol{q}\nu} \sum_{n'} \underbrace{|\langle \psi_{\boldsymbol{k}+\boldsymbol{q}n'} | H^{(1)}_{\boldsymbol{q}\nu} | \psi_{\boldsymbol{k}n} \rangle|^2}_{\text{matrix element}} \left[\frac{f_{\boldsymbol{k}+\boldsymbol{q},n'}}{\boxed{\varepsilon^0_{\boldsymbol{k}n} - \varepsilon^0_{\boldsymbol{k}+\boldsymbol{q}n'}} + \omega_{\boldsymbol{q}\nu} + i\delta} + \frac{1 - f_{\boldsymbol{k}+\boldsymbol{q},n'}}{\boxed{\varepsilon^0_{\boldsymbol{k}n} - \varepsilon^0_{\boldsymbol{k}+\boldsymbol{q}n'}} - \omega_{\boldsymbol{q}\nu} + i\delta} \right]$$

Computational framework:

DFT+DFPT, PBE-GGA, ElectronPhononCoupling python module (G. Antonius)

Including SOC : comparison to experiment

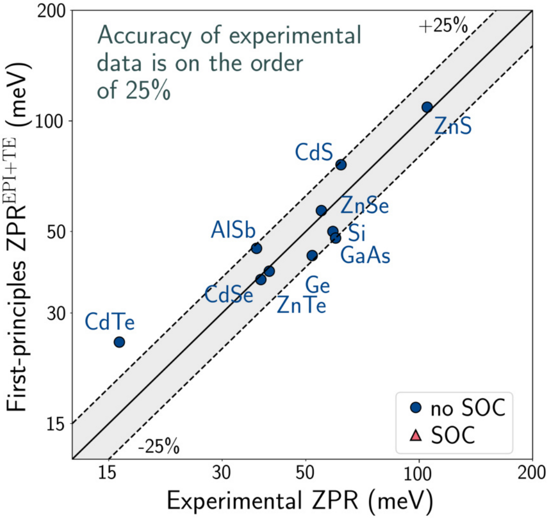

Including SOC : comparison to experiment

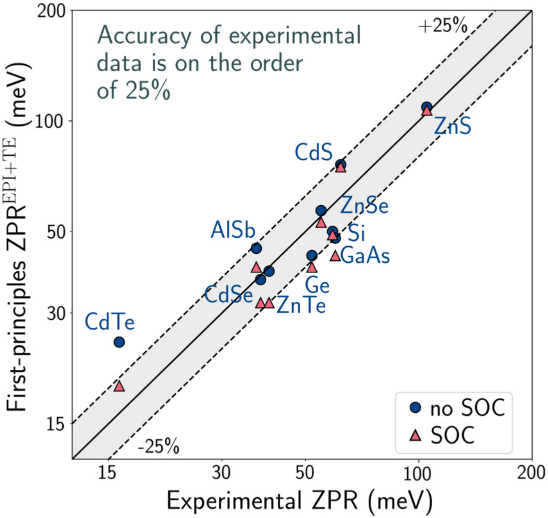

Including SOC : comparison to experiment

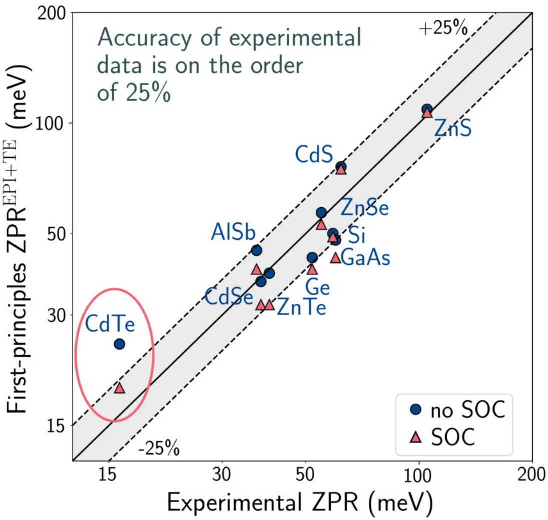

First-principles results: effect of SOC vs splitoff energy

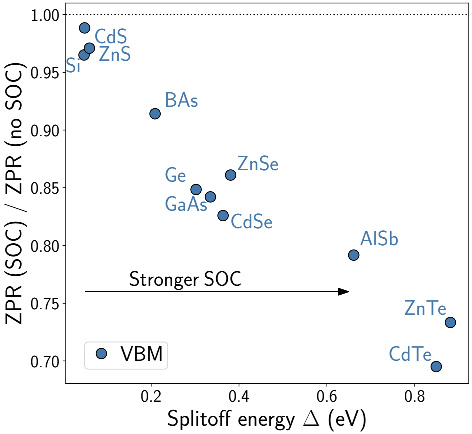

Stronger SOC

Valence band maximum

Material	Δ_{SO} (meV)	ω_{LO} (meV)	ZPR(noSOC) (meV)	ZPR(SOC) (meV)
Si	47	62.4	34.3	33.1
ZnS	60	40.6	48.1	46.7
CdS	49	34.4	43.3	41.7
BAs	209	84.4	45.5	41.5
Ge	302	38.7	16.5	14.0
GaAs	335	35.4	19.0	16.0
ZnSe	381	29.3	29.5	25.4
CdSe	364	23.6	24.7	20.3
AlSb	661	39.8	24.0	19.0
ZnTe	881	24.1	24.1	18.0
CdTe	849	19.1	16.4	11.4

First-principles results: mode decomposition

CdS: polar + weak SOC

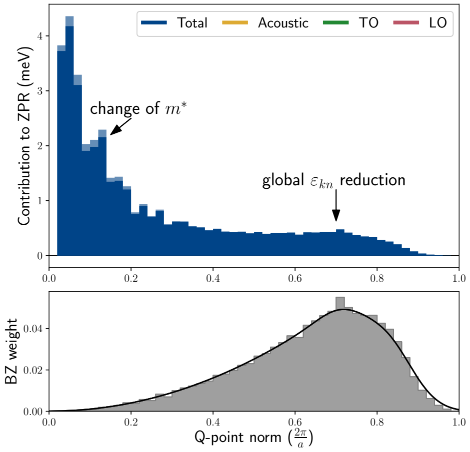

CdTe: polar + strong SOC

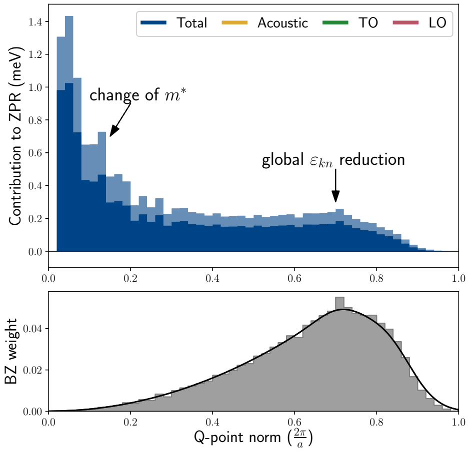

First-principles results: mode decomposition

CdS: polar + weak SOC

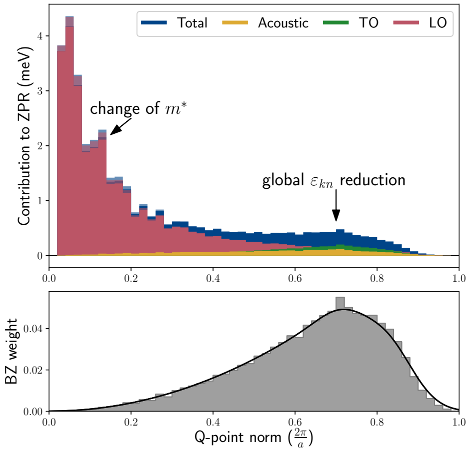

CdTe: polar + strong SOC

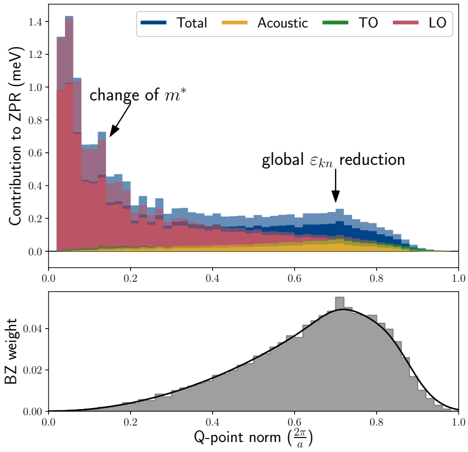

Fröhlich model

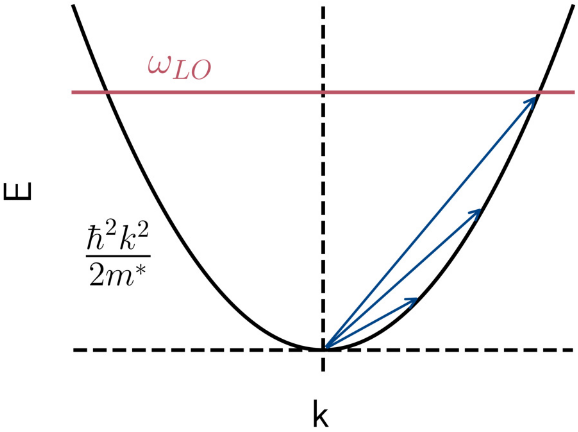

- Single electron in isotropic band
- Single Einstein phonon
- Polaron picture

$$\mathrm{ZPR}^{\mathrm{Fr}} = -\alpha\omega_{LO}$$

$$\alpha = \left(\frac{1}{\epsilon^{\infty}} - \frac{1}{\epsilon^{0}}\right)\sqrt{\frac{m^*}{2\omega_{LO}}}$$

Generalized Fröhlich model (gFr)

For valence band:

$$\mathrm{ZPR}_v^{\mathrm{Fan}} = \mathfrak{Re}\, \frac{1}{N_{\boldsymbol{q}}}\sum_{\boldsymbol{q}} \sum_{\nu} \overbrace{\boxed{\sum_{n=1}^{n_d}}}^{\text{Degenerate states}} \underbrace{|\langle\psi_{\boldsymbol{k}+\boldsymbol{q}n}|\, H^{(1)}_{\boldsymbol{q}\nu}\, |\psi_{\boldsymbol{k}v}\rangle|^2}_{\lim_{q\to 0}} \left[\underbrace{\frac{f_{\boldsymbol{k}+\boldsymbol{q},n}}{\varepsilon^0_{\boldsymbol{k}v} - \varepsilon^0_{\boldsymbol{k}+\boldsymbol{q}n} + \omega_{\boldsymbol{q}\nu} + i\delta}}_{\lim_{q\to 0}} + \cancel{\underbrace{\frac{1-f_{\boldsymbol{k}+\boldsymbol{q},n}}{\varepsilon^0_{\boldsymbol{k}v} - \varepsilon^0_{\boldsymbol{k}+\boldsymbol{q}n} - \omega_{\boldsymbol{q}\nu} + i\delta}}_{\text{unoccupied bands}}} \right]$$

$$\downarrow \qquad \downarrow$$

$$\mathrm{ZPR}_v^{\mathrm{gFr}} = \frac{\Omega_0}{(2\pi)^3}\int d^3q \sum_j \boxed{\sum_{n=1}^{n_d}} \underbrace{\frac{1}{q^2}\left(\frac{4\pi}{\Omega_0}\right)^2 \frac{|s_{nv}(\hat{\boldsymbol{q}})|^2}{2\omega_{j0}(\hat{\boldsymbol{q}})} \left(\frac{\hat{\boldsymbol{q}}\cdot \boldsymbol{p}_j(\hat{\boldsymbol{q}})}{\epsilon^\infty(\hat{\boldsymbol{q}})}\right)^2}_{\text{Dielectric interaction}} \left[\frac{1}{\frac{q^2}{2m_n^*(\hat{\boldsymbol{q}})} + \omega_{j0}(\hat{\boldsymbol{q}}) + \cancel{i\delta}}\right]$$

Miglio, Brousseau-Couture *et al.*, NPJ Computational Materials **6** 167 (2020)

Generalized Fröhlich model (gFr)

For valence band:

$$\mathrm{ZPR}_v^{\mathrm{Fan}} = \mathfrak{Re}\ \frac{1}{N_{\boldsymbol{q}}}\sum_{\boldsymbol{q}} \boxed{\sum_{\nu}} \overbrace{\boxed{\sum_{n=1}^{n_d}}}^{\text{Degenerate states}} \underbrace{|\langle\psi_{\boldsymbol{k}+\boldsymbol{q}n}|\, H^{(1)}_{\boldsymbol{q}\nu}\, |\psi_{\boldsymbol{k}v}\rangle|^2}_{\lim_{q\to 0}} \left[\underbrace{\frac{f_{\boldsymbol{k}+\boldsymbol{q},n}}{\varepsilon^0_{\boldsymbol{k}v} - \varepsilon^0_{\boldsymbol{k}+\boldsymbol{q}n} + \omega_{\boldsymbol{q}\nu} + i\delta}}_{\lim_{q\to 0}} + \cancel{\underbrace{\frac{1 - f_{\boldsymbol{k}+\boldsymbol{q},n}}{\varepsilon^0_{\boldsymbol{k}v} - \varepsilon^0_{\boldsymbol{k}+\boldsymbol{q}n} - \omega_{\boldsymbol{q}\nu} + i\delta}}_{\text{unoccupied bands}}}\right]$$

$$\mathrm{ZPR}_v^{\mathrm{gFr}} = \frac{\Omega_0}{(2\pi)^3}\int d^3q\ \underbrace{\boxed{\sum_{j}}}_{\text{LO}} \boxed{\sum_{n=1}^{n_d}} \underbrace{\frac{1}{q^2}\left(\frac{4\pi}{\Omega_0}\right)^2 \frac{|s_{nv}(\hat{\boldsymbol{q}})|^2}{2\omega_{j0}(\hat{\boldsymbol{q}})}\left(\frac{\hat{\boldsymbol{q}}\cdot\boldsymbol{p}_j(\hat{\boldsymbol{q}})}{\epsilon^\infty(\hat{\boldsymbol{q}})}\right)^2}_{\text{Dielectric interaction}} \left[\frac{1}{\frac{q^2}{2m_n^*(\hat{\boldsymbol{q}})} + \omega_{j0}(\hat{\boldsymbol{q}}) + \cancel{i\delta}}\right]$$

Miglio, Brousseau-Couture *et al.*, NPJ Computational Materials **6** 167 (2020)

Generalized Fröhlich model (gFr)

For valence band:

$$\mathrm{ZPR}_v^{\mathrm{Fan}} = \Re\mathfrak{e} \boxed{\frac{1}{N_{\mathbf{q}}}\sum_{\mathbf{q}}} \boxed{\sum_{\nu}} \overbrace{\boxed{\sum_{n=1}^{n_d}}}^{\text{Degenerate states}} \underbrace{|\langle\psi_{\mathbf{k}+\mathbf{q}n}|H^{(1)}_{\mathbf{q}\nu}|\psi_{\mathbf{k}v}\rangle|^2}_{\lim_{q\to 0}} \left[\underbrace{\frac{f_{\mathbf{k}+\mathbf{q},n}}{\varepsilon^0_{\mathbf{k}v} - \varepsilon^0_{\mathbf{k}+\mathbf{q}n} + \omega_{\mathbf{q}\nu} + i\delta}}_{\lim_{q\to 0}} + \cancel{\underbrace{\frac{1-f_{\mathbf{k}+\mathbf{q},n}}{\varepsilon^0_{\mathbf{k}v} - \varepsilon^0_{\mathbf{k}+\mathbf{q}n} - \omega_{\mathbf{q}\nu} + i\delta}}_{\text{unoccupied bands}}}\right]$$

$$\mathrm{ZPR}_v^{\mathrm{gFr}} = \boxed{\frac{\Omega_0}{(2\pi)^3}\int d^3q} \underbrace{\boxed{\sum_j}}_{\text{LO}} \boxed{\sum_{n=1}^{n_d}} \underbrace{\frac{1}{q^2}\left(\frac{4\pi}{\Omega_0}\right)^2 \frac{|s_{nv}(\hat{\mathbf{q}})|^2}{2\omega_{j0}(\hat{\mathbf{q}})}\left(\frac{\hat{\mathbf{q}}\cdot\mathbf{p}_j(\hat{\mathbf{q}})}{\epsilon^\infty(\hat{\mathbf{q}})}\right)^2}_{\text{Dielectric interaction}} \left[\frac{1}{\frac{q^2}{2m_n^*(\hat{\mathbf{q}})} + \omega_{j0}(\hat{\mathbf{q}}) + \cancel{i\delta}}\right]$$

Miglio, Brousseau-Couture *et al.*, NPJ Computational Materials **6** 167 (2020)

Generalized Fröhlich model (gFr)

For valence band:

$$\mathrm{ZPR}_v^{\mathrm{Fan}} = \mathfrak{Re}\, \boxed{\frac{1}{N_{\boldsymbol{q}}}\sum_{\boldsymbol{q}}}\, \boxed{\sum_{\nu}}\, \overbrace{\boxed{\sum_{n=1}^{n_d}}}^{\text{Degenerate states}} \underbrace{|\langle\psi_{\boldsymbol{k}+\boldsymbol{q}n}|\, H^{(1)}_{\boldsymbol{q}\nu}\, |\psi_{\boldsymbol{k}v}\rangle|^2}_{\lim_{q\to 0}} \left[\underbrace{\frac{f_{\boldsymbol{k}+\boldsymbol{q},n}}{\varepsilon^0_{\boldsymbol{k}v} - \varepsilon^0_{\boldsymbol{k}+\boldsymbol{q}n} + \omega_{\boldsymbol{q}\nu} + i\delta}}_{\lim_{q\to 0}} + \cancel{\underbrace{\frac{1 - f_{\boldsymbol{k}+\boldsymbol{q},n}}{\varepsilon^0_{\boldsymbol{k}v} - \varepsilon^0_{\boldsymbol{k}+\boldsymbol{q}n} - \omega_{\boldsymbol{q}\nu} + i\delta}}_{\text{unoccupied bands}}} \right]$$

$$\downarrow$$

$$\mathrm{ZPR}_v^{\mathrm{gFr}} = \boxed{\frac{\Omega_0}{(2\pi)^3}\int d^3q}\, \underbrace{\boxed{\sum_{j}}}_{\text{LO}}\, \boxed{\sum_{n=1}^{n_d}}\, \underbrace{\frac{1}{q^2}\left(\frac{4\pi}{\Omega_0}\right)^2 \frac{|s_{nv}(\hat{\boldsymbol{q}})|^2}{2\omega_{j0}(\hat{\boldsymbol{q}})} \left(\frac{\hat{\boldsymbol{q}}\cdot\boldsymbol{p}_j(\hat{\boldsymbol{q}})}{\epsilon^\infty(\hat{\boldsymbol{q}})}\right)^2}_{\text{Dielectric interaction}} \left[\frac{1}{\boxed{\frac{q^2}{2m_n^*(\hat{\boldsymbol{q}})}} + \omega_{j0}(\hat{\boldsymbol{q}}) + \cancel{i\delta}}\right]$$

Assumptions: dispersionless LO phonon, **parabolic electronic band around extrema**

Miglio, Brousseau-Couture *et al.*, NPJ Computational Materials **6** 167 (2020)

Generalized Fröhlich model (gFr)

For valence band:

$$\mathrm{ZPR}_v^{\mathrm{Fan}} = \Re\mathfrak{e} \boxed{\frac{1}{N_{\boldsymbol{q}}}\sum_{\boldsymbol{q}}} \boxed{\sum_{\nu}} \overbrace{\boxed{\sum_{n=1}^{n_d}}}^{\text{Degenerate states}} \underbrace{|\langle\psi_{\boldsymbol{k}+\boldsymbol{q}n}| H^{(1)}_{\boldsymbol{q}\nu} |\psi_{\boldsymbol{k}v}\rangle|^2}_{\lim_{q\to 0}} \left[\underbrace{\frac{f_{\boldsymbol{k}+\boldsymbol{q},n}}{\varepsilon^0_{\boldsymbol{k}v} - \varepsilon^0_{\boldsymbol{k}+\boldsymbol{q}n} + \omega_{\boldsymbol{q}\nu} + i\delta}}_{\lim_{q\to 0}} + \cancel{\underbrace{\frac{1-f_{\boldsymbol{k}+\boldsymbol{q},n}}{\varepsilon^0_{\boldsymbol{k}v} - \varepsilon^0_{\boldsymbol{k}+\boldsymbol{q}n} - \omega_{\boldsymbol{q}\nu} + i\delta}}_{\text{unoccupied bands}}} \right]$$

$$\mathrm{ZPR}_v^{\mathrm{gFr}} = \boxed{\frac{\Omega_0}{(2\pi)^3}\int d^3q} \underbrace{\boxed{\sum_{j}}}_{\text{LO}} \boxed{\sum_{n=1}^{n_d}} \underbrace{\frac{1}{q^2}\left(\frac{4\pi}{\Omega_0}\right)^2 \frac{|s_{nv}(\hat{\boldsymbol{q}})|^2}{2\omega_{j0}(\hat{\boldsymbol{q}})} \left(\frac{\hat{\boldsymbol{q}}\cdot\boldsymbol{p}_j(\hat{\boldsymbol{q}})}{\epsilon^\infty(\hat{\boldsymbol{q}})}\right)^2}_{\text{Dielectric interaction}} \left[\frac{1}{\boxed{\frac{q^2}{2m_n^*(\hat{\boldsymbol{q}})}} + \omega_{j0}(\hat{\boldsymbol{q}}) + \cancel{i\delta}}\right]$$

Assumptions: dispersionless LO phonon, **parabolic electronic band around extrema**

... now, do the radial integral in $\int d^3q$ ...

Miglio, Brousseau-Couture *et al.*, NPJ Computational Materials **6** 167 (2020)

SOC effect on generalized Fröhlich ZPR

$$\mathrm{ZPR}_v^{gFr} = \sum_{j,n} \frac{1}{\sqrt{2}\Omega_0} \boxed{\frac{1}{n_d}} \int_{4\pi} d\hat{\boldsymbol{q}} \boxed{\left(m_n^*(\hat{\boldsymbol{q}})\right)^{1/2}} \left(\omega_{j0}(\hat{\boldsymbol{q}})\right)^{-3/2} \left(\frac{\hat{\boldsymbol{q}}.\boldsymbol{p}_j(\hat{\boldsymbol{q}})}{\epsilon^\infty(\hat{\boldsymbol{q}})}\right)^2.$$

Simplified picture for zincblende structure:

$$\mathrm{ZPR}_v^{gFr} \propto \text{average of} \int_{4\pi} d\hat{\boldsymbol{q}} (m^*)^{\frac{1}{2}} \qquad [1]$$

SOC effect on Fröhlich ZPR captured by the **change in angular-averaged effective masses**

$$\text{Valence:} \quad \frac{\mathrm{ZPR}_v(\mathrm{SOC})}{\mathrm{ZPR}_v(\mathrm{noSOC})} \approx \frac{\frac{1}{2}\left(\langle m_{hh}^*(\mathrm{SOC})^{\frac{1}{2}}\rangle + \langle m_{lh}^*(\mathrm{SOC})^{\frac{1}{2}}\rangle\right)}{\frac{1}{3}\left(2\langle m_{hh}^*(\mathrm{noSOC})^{\frac{1}{2}}\rangle + \langle m_{lh}^*(\mathrm{noSOC})^{\frac{1}{2}}\rangle\right)}$$

[1] G.D. Mahan, J. Phys. Chem. Solids 26 (1965)

SOC effect within Luttinger-Kohn model

First-principles	???	Generalized Fröhlich model
EPI interaction + SOC : NC pseudos only	$\Longleftrightarrow$	$\langle m^* \rangle$ from DFPT + SOC : PAW only

SOC effect within Luttinger-Kohn model

First-principles	???	Generalized Fröhlich model
EPI interaction + SOC : NC pseudos only	$\Longleftrightarrow$	$\langle m^* \rangle$ from DFPT + SOC : PAW only

Luttinger-Kohn Hamiltonian without SOC :

$$H_{n,n'}(\boldsymbol{k}) = \begin{bmatrix} Ak_x^2 + B(k_y^2 + k_z^2) & Ck_x k_y & Ck_x k_z \\ Ck_x k_y & Ak_y^2 + B(k_x^2 + k_z^2) & Ck_y k_z \\ Ck_x k_y & Ck_y k_z & Ak_z^2 + B(k_x^2 + k_y^2) \end{bmatrix}$$

A, B, C : Luttinger parameters
(2^{nd} order $\boldsymbol{k} \cdot \boldsymbol{p}$)
(optdriver 7, eph_task 6, no SOC, band extrema with $n_{deg} = 3$)

6 band LK model with SOC:

- Input parameters: A, B, C and Δ_{SO}
- $\{|j, m_j\rangle\}$ basis
- Solve dispersion for h.h. and l.h. bands
- $\langle m^* \rangle$ from finite differences

Relating gFr to first-principles: VBM

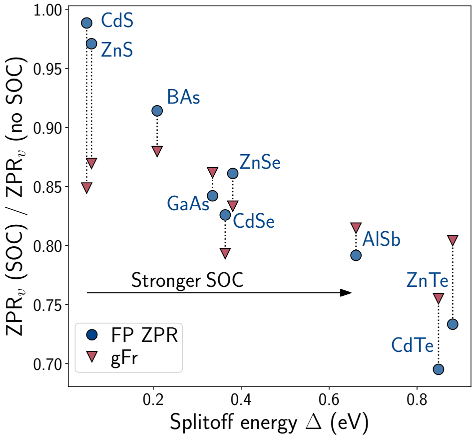

Valence band maximum

Stronger SOC

Material	Δ_{SO} (meV)	ω_{LO} (meV)	ZPR(SOC)/ZPR(noSOC)		
			FP	**FP LO**	**gFr**
ZnS	60	40.6	0.97	0.95	0.87
CdS	49	34.4	0.96	0.96	0.85
BAs	209	84.4	0.91	0.94	0.88
GaAs	335	35.4	0.84	0.88	0.86
ZnSe	381	29.3	0.86	0.88	0.83
CdSe	364	23.6	0.83	0.83	0.79
AlSb	661	39.8	0.79	0.82	0.82
ZnTe	881	24.1	0.73	0.79	0.81
CdTe	849	19.1	0.69	0.74	0.76

Relating gFr to first-principles: VBM

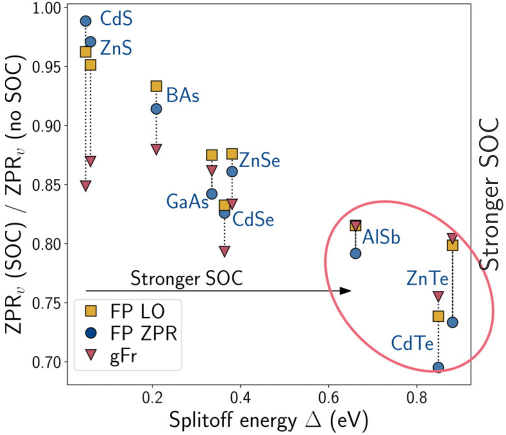

Valence band maximum

Stronger SOC

Material	Δ_{SO} (meV)	ω_{LO} (meV)	ZPR(SOC)/ZPR(noSOC)		
			FP	**FP LO**	**gFr**
ZnS	60	40.6	0.97	0.95	0.87
CdS	49	34.4	0.96	0.96	0.85
BAs	209	84.4	0.91	0.94	0.88
GaAs	335	35.4	0.84	0.88	0.86
ZnSe	381	29.3	0.86	0.88	0.83
CdSe	364	23.6	0.83	0.83	0.79
AlSb	661	39.8	0.79	0.82	0.82
ZnTe	881	24.1	0.73	0.79	0.81
CdTe	849	19.1	0.69	0.74	0.76

Relating gFr to first-principles: VBM

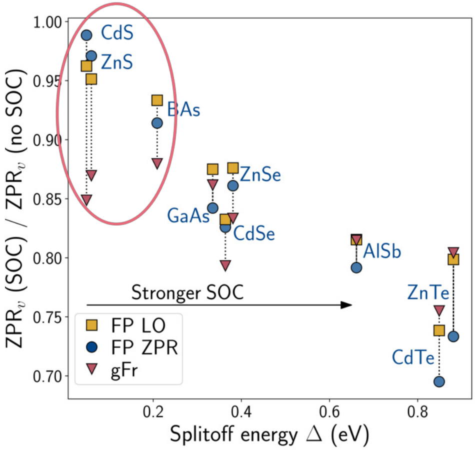

Stronger SOC

Valence band maximum

Material	Δ_{SO} (meV)	ω_{LO} (meV)	ZPR(SOC)/ZPR(noSOC)		
			FP	**FP LO**	**gFr**
ZnS	60	40.6	0.97	0.95	0.87
CdS	49	34.4	0.96	0.96	0.85
BAs	209	84.4	0.91	0.94	0.88
GaAs	335	35.4	0.84	0.88	0.86
ZnSe	381	29.3	0.86	0.88	0.83
CdSe	364	23.6	0.83	0.83	0.79
AlSb	661	39.8	0.79	0.82	0.82
ZnTe	881	24.1	0.73	0.79	0.81
CdTe	849	19.1	0.69	0.74	0.76

Validity of the effective mass approximation

Radial integral has analytic solution:

$$\int_0^\infty dq \frac{1}{\frac{q^2}{2m^*} + \omega_{\mathrm{LO}}} \Rightarrow \int_0^\infty dq \frac{1}{Aq^2 + B} = \frac{1}{\sqrt{AB}} \frac{\pi}{2}$$

Effective mass approximation holds for
only $\sim$ 10%**(l.h.)** - 20%**(h.h)** **of BZ**

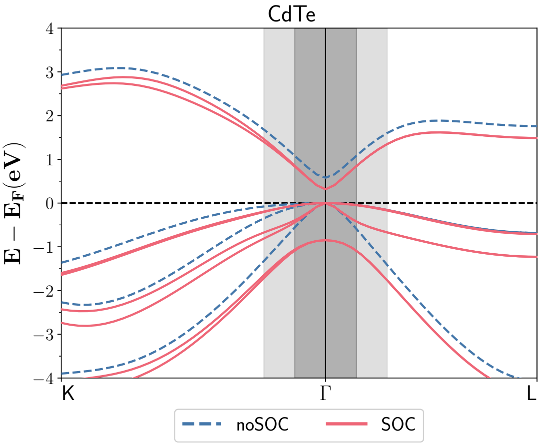

Validity of the effective mass approximation

For finite upper bound:

$$\int_0^{q_c} dq \frac{1}{Aq^2 + B} = \sqrt{\frac{1}{AB}} \mathrm{Arctan}\left(q_c \sqrt{\frac{A}{B}}\right)$$

$$A = (2m^*)^{-1}, \quad B = \omega_{\mathrm{LO}}$$

Evaluate at smallest q_c at which parabolicity is lost:

- Most materials: $60-80\%$ of asymptotic limit (lower bound)
- Breakdown of parabolic approx. when $\omega_{LO} \sim \Delta_{\mathrm{SO}}$

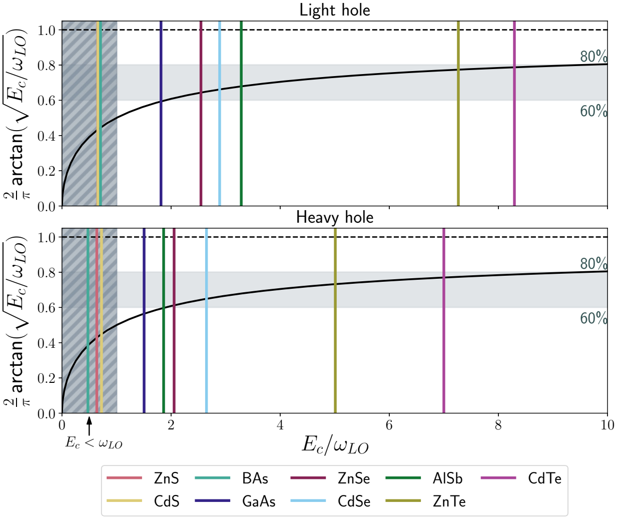

Conclusion and outlook

Summary

- We study SOC effect of ZPR from first-principles for 11 benchmark semiconductors
- ZPR decrease originates from both global lowering of $\varepsilon_{\boldsymbol{k}n}$ (large q, all modes) and effective masses modification (small q, LO)
- Simplified effective mass model based on generalized Fröhlich model gives correct trends, but fails quantitatively when $\omega_{\text{LO}} \sim \Delta_{\text{SO}}$

Outlook

- Implement gFr model + SOC using finite differences from *ab initio* dispersion for $\langle m^* \rangle$
- Investigate effect of SOC on $|gkk|^2$ vs $\varepsilon^0_{\boldsymbol{k}n}$

Conclusion and outlook

Summary

- We study SOC effect of ZPR from first-principles for 11 benchmark semiconductors
- ZPR decrease originates from both global lowering of $\varepsilon_{\boldsymbol{k}n}$ (large q, all modes) and effective masses modification (small q, LO)
- Simplified effective mass model based on generalized Fröhlich model gives correct trends, but fails quantitatively when $\omega_{\text{LO}} \sim \Delta_{\text{SO}}$

Thank you for your attention!

NSERC CRSNG

Calcul Québec

compute canada | calcul canada

Fonds de recherche Nature et technologies Québec

Hydro Québec

Abinit